

# NEURAL FOURIER SHIFT FOR BINAURAL SPEECH RENDERING

Jin Woo Lee, Kyogu Lee

Department of Intelligence and Information, Seoul National University

{jinwlee, kglee}@snu.ac.kr

## ABSTRACT

We present a neural network for rendering binaural speech from given monaural audio, position, and orientation of the source. Most of the previous works have focused on synthesizing binaural speeches by conditioning the positions and orientations in the feature space of convolutional neural networks. These synthesis approaches are powerful in estimating the target binaural speeches even for in-the-wild data but are difficult to generalize for rendering the audio from out-of-distribution domains. To alleviate this, we propose Neural Fourier Shift (NFS), a novel network architecture that enables binaural speech rendering in the Fourier space. Specifically, utilizing a geometric time delay based on the distance between the source and the receiver, NFS is trained to predict the delays and scales of various early reflections. NFS is efficient in both memory and computational cost, is interpretable, and operates independently of the source domain by its design. With up to 25 times lighter memory and 6 times fewer calculations, the experimental results show that NFS outperforms the previous studies on the benchmark dataset.

**Index Terms**— Binaural speech synthesis, binaural rendering, spatial audio, neural network

## 1. INTRODUCTION

Binaural audio synthesis is an essential technology for providing immersive sound experiences in virtual and extended reality. By simulating the precise clues to locate the sound source, binaural sound synthesis aims to provide a spatial experience to our auditory cues [1], which is also known as spatial hearing. Rendering spatialized audio from arbitrary sounds with low computational cost and high quality is an essential technology in AR/VR platforms.

Humans can localize sounds using a variety of perceptual cues, including Interaural Time Difference (ITD), Interaural Intensity Difference (IID), and spectral distortions caused by interactions with the listener’s pinnae, head, and torso [2, 3, 4]. Such cues can implicitly be modeled using head-related impulse response (HRIR) and binaural room impulse response (BRIR) [5, 6]. Traditional approaches for binaural audio rendering relied on digital signal processing (DSP) theories to model the HRIRs, BRIRs, or ambient noises [7, 8, 9, 10]. Most of these approaches model the binaural environments based on the linear time-invariant (LTI) system, and some difficulties have been discussed that such methods are insufficient for accurately modeling the real-world acoustic nonlinearities [11].

While pointing out such limitations, recent studies utilize neural networks on binaural speech synthesis [12, 13]. By conditioning

Sound samples of *speech*, *singing*, *music*, and *noise* are available at: <https://bit.ly/3Sy6iFa>

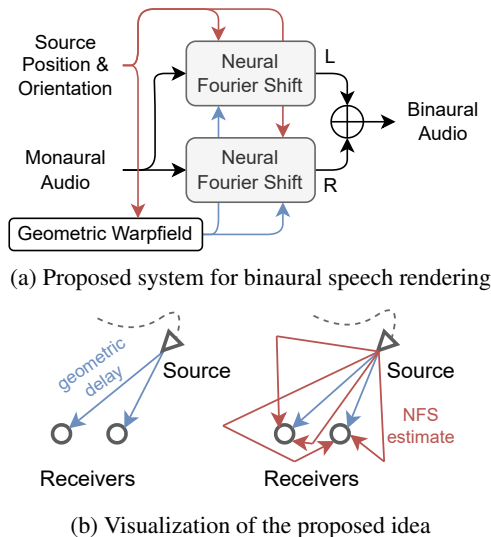


**Fig. 1.** Schematic illustration of the proposed system and rough visualization of the modeled acoustic paths. Utilizing geometric delays that reflect only the shortest path between the source and receiver, our model predicts other possible early reflections.

the positions and orientations in the feature space of convolutional neural networks, the neural network approaches synthesize the binaural speeches as raw waveforms. These synthesis approaches are powerful in estimating the distribution of target real-world binaural speeches, but it is difficult to generalize for rendering the audio from out-of-distribution domains such as music, or general sound events.

In this paper, we propose a novel neural network that can render the binaural speech independent of the source domain, based on the theoretical foundation of DSP. We start from the idea to use the delays that can be computed from geometric distances as bases for early reflections. Such delay can be considered equivalent to the ‘Geometric Warfield’ of [12], which represents the phase lag in the acoustic path arriving at the shortest of many possible paths between the source and receiver. Based on the computed shortest delay, we aim to further predict the possible early reflections and model the responses. We summarize our contributions as follows:

- We propose a model for binaural speech rendering, which is highly efficient in memory and computational cost, and is also interpretable.
- We empirically show that our method outperforms the previous studies in quantitative measures.
- Perceptual evaluation shows the effect of the proposed architecture, along with the performance comparison.

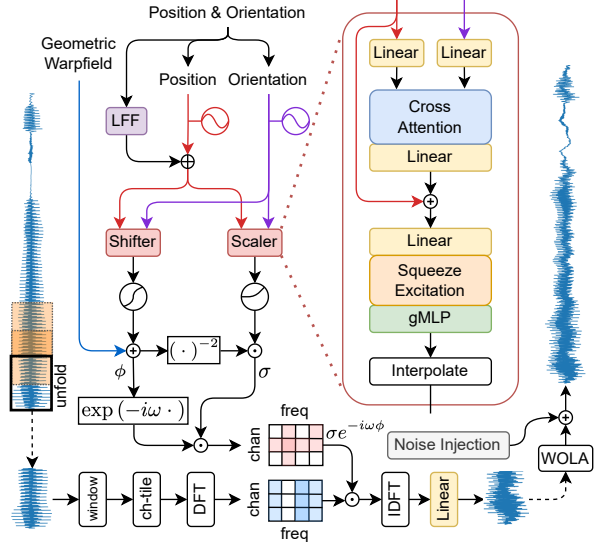


**Fig. 2.** Architecture of NFS. Dashed arrows represent frame-wise segmentation or collection. `ch-tilde` indicates channel-wise repetition. Every `Linear` indicates a channel-wise linear operation.

## 2. RELATED WORKS

Traditionally, signal processing technology has long laid the foundation for binaural audio synthesis [7, 8, 9]. However, more recent studies utilize deep learning to solve binaural speech synthesis in an end-to-end manner [12, 13, 14]. Although these data-driven approaches are powerful in estimating the target binaural speech, even for the in-the-wild binaural recordings, they are inherently limited to estimating the distribution of the training set. Consequently, they are prone to failure in generalizations and may require other models to render out-of-domain data, which can be a disadvantage when considering on-device inference scenarios.

This situation naturally leads to the parameter estimation method as a way to utilize the powerful estimation ability of the neural network without being limited to the data domain. Lee *et al.* [15] showed that artificial reverberation parameters can be estimated in an end-to-end manner. They showed that neural networks can capture the target reverberation precisely in both analysis-synthesis and blind estimation tasks, outperforming the non-end-to-end approaches. Focusing on the spatial audio, Gebru *et al.* [16] implicitly approximated HRTFs using a neural network. More recent work by Richard *et al.* [17] proposed a framework for training neural networks to estimate IRs for the given position. Their proposed IR-MLP efficiently estimate the IRs and even learns the IRs from an in-the-wild binaural dataset, but there is room for performance improvement as the authors discussed in their paper.

Fourier transforms have historically had a significant impact on engineering advances and are often used to improve the performance of deep learning techniques. Fourier space is used for proving that the neural networks are universal approximators [18], and the transform advantages efficient computation of the neural convolutional layers [19]. More recently, Fourier transforms and sinusoidal activations are reported to benefit neural networks in solving kernel regression or inverse problems [20, 21]. Neural operators also benefit from the capability to learn parametric dependence to the solution of partial differential equations in quasi-linear time complexity, when defined in Fourier space [22].

## 3. PROPOSED METHOD

This work mainly focuses on modeling the binaural speech using a neural network, with an emphasis on time delay and energy reduction. While propagating through the air, sound has a delay in its arrival, and the energy is altered mainly due to attenuation and absorption. We introduce a novel network that models the delay and the energy reduction of the binaural speech in the Fourier space.

### 3.1. Neural Fourier Shift

For any  $\mathbf{x} \in \mathbb{R}^N$ , define the spectrum of  $\mathbf{x}$  by the Discrete Fourier Transform (DFT)  $\mathbf{X}[k] := \text{DFT}(\mathbf{x})[k] = \sum_{m=0}^{N-1} \mathbf{x}[m] e^{-i\omega_k m}$ , where  $\omega_k = 2\pi k/N$  for  $k = 0, 1, \dots, N-1$ . The spectrum of  $\text{SHIFT}_\Delta(\mathbf{x})$ , which is  $\mathbf{x}$  shifted for  $\Delta \in \mathbb{N}$ , satisfies

$$\text{DFT}(\text{SHIFT}_\Delta(\mathbf{x}))[k] = e^{-i\omega_k \Delta} \mathbf{X}[k]. \quad (1)$$

The equation (1) is also well known as the (Fourier) shift theorem, which implies that a delay of  $\Delta$  samples in the time corresponds to a linear phase term  $e^{-i\omega_k \Delta}$  in the frequency domain. The proposed method models the delay for early reflections by estimating the phase term. In addition to the linear time shift where the spectral magnitude remains unaffected, we aim to model the magnitude change from the monaural to the binaural speech.

Let  $\mathbf{X} \in \mathbb{C}^N$  be the spectrum of a monaural speech  $\mathbf{x}$ , and suppose that the source's position  $p \in \mathbb{R}^3$  and the orientation  $q \in \mathbb{R}^4$  are given. We introduce a neural network  $\Psi_\theta : (p, q) \mapsto (\sigma_L, \phi_L, \sigma_R, \phi_R)$  with parameter  $\theta$  to estimate the magnitude change  $\sigma \in \mathbb{R}^{C \times N}$  and the phase shift  $\phi \in \mathbb{R}^{C \times N}$  with  $C$  number of channels for left (L) and right (R) ears. The estimated output shifts the monaural speech by  $\phi$  and scales by  $\sigma$  using the equation (1), which can be expressed as

$$\begin{aligned} \hat{\mathbf{X}}_L[k] &= \sum_{c=0}^{C-1} \sigma_L[c, k] e^{-i\omega_k \phi_L[c, k]} \mathbf{X}[k], \\ \hat{\mathbf{X}}_R[k] &= \sum_{c=0}^{C-1} \sigma_R[c, k] e^{-i\omega_k \phi_R[c, k]} \mathbf{X}[k], \end{aligned} \quad (2)$$

The binaural spectrum is then obtained by a concatenation as  $\hat{\mathbf{X}} = \hat{\mathbf{X}}_L \oplus \hat{\mathbf{X}}_R$ . The binaural speech  $\hat{\mathbf{x}}$  is finally estimated by imposing the inverse DFT (IDFT) to the  $\hat{\mathbf{X}}$ . By design,  $\Psi_\theta$  estimates the frame-wise multichannel spectrum independent of the source spectrum.

For given binaural recording  $\mathbf{y}$  of monaural speech  $\mathbf{x}$ , the neural network  $\Psi_\theta$  is trained to minimize the loss between  $\hat{\mathbf{x}}$  and  $\mathbf{y}$  as

$$\begin{aligned} \mathcal{L}(\hat{\mathbf{x}}, \mathbf{y}) &= \lambda_1 \underbrace{\|\hat{\mathbf{x}} - \mathbf{y}\|_2}_{\ell_2} + \lambda_2 \underbrace{\|\angle \hat{\mathbf{X}} - \angle \mathbf{Y}\|_1}_{\mathcal{L}_{\text{phs}}} \\ &+ \lambda_3 \underbrace{\|\text{IID}(\hat{\mathbf{x}}) - \text{IID}(\mathbf{y})\|_2}_{\mathcal{L}_{\text{IID}}} + \lambda_4 \underbrace{\|\text{MRSTFT}(\hat{\mathbf{x}}, \mathbf{y})\|_1}_{\mathcal{L}_{\text{STFT}}}, \end{aligned} \quad (3)$$

where we define the IID as the mean of the interaural difference between the log magnitudes of the left and right spectrums

$$\text{IID}(\mathbf{x}) := \frac{1}{M} \sum_{k=0}^M \log_{10} |\mathbf{X}_L[k]| - \log_{10} |\mathbf{X}_R[k]|, \quad (4)$$

MRSTFT stands for the multi-resolution STFT loss [23], and  $\lambda_i$  are the hyperparameters.  $\mathcal{L}_{\text{phs}}$  denotes the angular phase error, which Richard *et al.* [12] proved advantageous in overcoming the deficiencies of optimization through  $\ell_2$ -loss between the waveforms.

Model	$\ell_2 \cdot 10^3$	Amp.	$\mathcal{L}_{\text{phs}}$	PESQ	$\mathcal{L}_{\text{STFT}}$
WaveNet [24]	0.179	0.037	0.968	2.305	1.915
IR-MLP [17]	0.236	0.042	0.933	-	-
WarpNet [12]	0.167	0.048	<b>0.807*</b>	-	-
WarpNet <sup>◊</sup> [13]	<b>0.157<sup>†</sup></b>	0.038	0.838	<b>2.360<sup>†</sup></b>	1.774
BinauralGrad [13]	<b>0.128*</b>	<b>0.030*</b>	<b>0.837<sup>†</sup></b>	<b>2.759*</b>	1.278
<b>Ours (NFS)</b>	0.172	<b>0.035<sup>†</sup></b>	0.999	1.656	<b>1.241*</b>
wo.NI	0.172	<b>0.035<sup>†</sup></b>	0.959	1.651	2.280
wo.LFF	0.207	0.037	1.118	1.592	1.267
wo.GeoWarp	0.197	<b>0.035<sup>†</sup></b>	1.200	1.681	<b>1.248<sup>†</sup></b>
wo.Shifter	0.433	0.039	1.570	1.502	1.288

**Table 1.** Quantitative results. The highest score for each metric is marked with an asterisk (\*), and the second highest score is marked with a dagger (<sup>†</sup>). WarpNet<sup>◊</sup> shows results reported by [13].

### 3.2. Network Architecture

As illustrated in Figure 1, NFS takes three inputs: monaural audio, the source’s position with orientation, and frame-wise geometric delay. First of all, the monaural audio is chunked into frames with overlaps, where we call it as `unfold`. Using the position and the orientation of the source, NFS binauralize each frame in the Fourier space, following the formulations in Section 3.1. We illustrate the schematic network architecture of NFS in Figure 2.

The position and the orientation of the source are encoded using sinusoidal encoding and learned Fourier features (LFF) [20]. We estimate the framewise frequency response  $\sigma$  and phase delay  $\phi$  using the neural networks named as `Scaler` and `Shifter`, respectively. The architecture of `Scaler` and `Shifter` is the same, which consists of cross-attention [25], squeeze-and-excitation [26], gMLP [27], and channel-wise linear layers as the trainable modules.

Cross-attention fuses information of two separate embeddings using attention mechanism [25]. Putting the embeddings of the source positions as query and those of the orientations as key and value, the cross-attention layer conditionally fuses the orientation to the positional information. The position embedding is added to the cross-attention output by a residual connection. A channel-wise linear layer follows to project the embedding to a higher dimensional space with `chan` number of channels (which is the same number of channels that we repeat the source during `ch-tile`).

Squeeze-and-excitation then extracts informative features by fusing spatial and channel-wise information [26]. gMLP is a variation of MLP which can be a simple alternative to the multi-head self-attention layers in Transformers [25, 27]. Equipped with a spatial gating unit, gMLP captures spatial information across embeddings. The output of gMLP is then linearly interpolated to `freq` number of dimension to represent the scales (for `Scaler`) or the shifts (for `Shifter`) for the `freq` number of frequency bins. The outputs of `Scaler` and `Shifter` are then transformed through non-linear activations, where we denote by  $\varphi := \text{Sigmoid}(\text{Shifter}) \in \mathbb{R}^{\text{chan} \times \text{freq}}$  and  $\varsigma := \text{Softplus}(\text{Scaler}) \in \mathbb{R}^{\text{chan} \times \text{freq}}$ . The transformation is intended to enforce  $\varsigma$  to be positive definite, and  $\varphi$  to be in a millisecond no larger than half of the frame length.

The `Shifter` output is biased by the geometric delay (given by a scalar  $g \in \mathbb{R}$  given for each frame) computed from the geometric warfield. We denote the biased shift by  $\phi = \varphi + g$ . To enforce the energy to be inversely proportional to the power of distance, we divide the `Scaler` output by  $\phi^2$  (since  $\phi$  is proportional to the distance), to compute the scale  $\sigma = \varsigma \odot \phi^{-2}$ . Finally we acquire the frame-wise multichannel spectrum  $\sigma \exp(-i\omega\phi) \in \mathbb{C}^{\text{chan} \times \text{freq}}$ , and multiply it to the source in the Fourier space as equation (2).

After the estimated  $\hat{\mathbf{X}} \in \mathbb{C}^{\text{chan} \times \text{freq}}$  is inverted back into the waveform using IDFT, we linearly project the channels into a single stem. We enforce the linear projection weights to be positive definite to make the projection independent of the phase shift. Indeed,  $\sigma \exp(-i\omega\phi)$  contains channel-wise IRs for each frame, where each channel can represent an IR for each different trajectory of acoustic rays. The NFS output frames are then synthesized using Weighted Overlap-add (WOLA) method. About the effect of each network module, we elaborate in more details based on the empirical observations in section 4.1.

### 3.3. Training Details

For each NFS responsible for left and right channels, we set both the number of channels `chan` and the number of dimensions for sinusoidal encoding to be 128. Our model is trained using RADam optimizer [28] for 16 epochs with a batch size of 6 where we randomly sample 800 ms of mono audio and the corresponding conditions for each batch. We train NFS with 200 ms frame length and 100 ms hop length, and the input with 800 ms mono audio is padded and chunked into 9 frames. While training NFS, regarding each frame as an independent batch, we stack the frames in batch dimension and estimate the output for all of the 9 frames in a single forward process. The learning rate was initialized by  $10^{-3}$  and scaled by the factor of 0.9 for every epoch. We set  $\lambda_1 = 10^3$ ,  $\lambda_3 = 10^1$ , and  $\lambda_2 = \lambda_4 = 1$ .

## 4. EVALUATION

We use the binaural speech benchmark dataset [12] for all experiments, which contains monaural-binaural paired audio data for approximately 2 hours long, with 48 kHz sampling rate. The binaural audio that the dataset provides is recorded using a KEMAR mannequin in a regular room, for the source speeches spoken by eight different subjects. The position and orientation of the source are tracked at 120 Hz and are aligned with the audio.

We use WarpNet<sup>1</sup> [12] and BinauralGrad<sup>2</sup> [13] as the baselines of the comparison to evaluate our model. The work by Huang *et al.* [14] was not included in the comparison because of the different training data. We compare our model with 6-layer IR-MLP [17] model with 512 hidden units they used for their experiment in training with the benchmark dataset. We also evaluate four variants of NFS: (1) NFS trained with Noise Injection but inference without it denoted by `wo.NI`, (2) our network trained without learned Fourier features denoted by `wo.LFF`, (3) our network trained without the time shift denoted by `wo.Shifter`, and (4) our network trained without Geometric Warfield denoted by `wo.GeoWarp`.

### 4.1. Quantitative Evaluation

Table 1 compares the objective results of each model for the binaural speech synthesis benchmark test set. `Amp.` denotes the (spectral) amplitude error [12]. NFS records the best MRSTFT score ( $\mathcal{L}_{\text{STFT}}$ ) and the second-best amplitude error compared to baselines. **Absence of noise injection** degrades the MRSTFT score of the NFS. As the `NI` module is intended to model ambient noise, inference results of NFS without it (denoted as `wo.NI`) show higher  $\mathcal{L}_{\text{STFT}}$  than the original NFS. However, for all other metrics, the model `wo.NI`

<sup>1</sup><https://github.com/facebookresearch/BinauralSpeechSynthesis/releases/tag/v1.1>

<sup>2</sup><https://github.com/microsoft/NeuralSpeech/tree/master/BinauralGrad#pretrained-models>

Model	# Param.	MACs ( $\downarrow$ )
BinauralGrad (stage 1, single step) [13]	6.91 M	229.4 G
BinauralGrad (stage 2, single step) [13]	6.91 M	229.3 G
WarpNet [12]	8.59 M	19.15 G
IR-MLP [17]	1.62 M	-
<b>Ours (NFS)</b>	<b>0.55 M</b>	<b>3.400 G</b>
wo.Shifter	<b>0.28 M</b>	<b>1.700 G</b>

**Table 2.** Comparison of memory and computational cost.

also records a similar performance to the original NFS – which implies that NFS learns to scale and shift the source independently of the ambient noise. **Learned Fourier features** slightly advantages NFS to encode the conditions, since `wo.LFF` performs worse than NFS in every measure. However, we emphasize that the performance of `wo.LFF` for  $\mathcal{L}_{\text{STFT}}$  is still better than that of BinauralGrad. **Without Shifter**, our network performs worse than the original NFS. `wo.Shifter` can only adjust the frequency response for each channel where all phases are uniformly shifted by the geometric delay. The absence of `Shifter` degrades especially for the  $\ell_2$ -loss and the angular phase error, and this shows the impact of the phase shift by `Shifter`. **Without geometric delay**, NFS predicts both the early reflections and the direct arrivals. Quantitative results show that `wo.GeoWarp` also performs similarly to NFS, but is slightly worse in  $\mathcal{L}_{\text{phs}}$ . As it appears in Figure 4, the relation between the input positions and the most dominant response estimated from `wo.GeoWarp` shows similar dynamics to that of NFS. It turns out that biasing  $\varphi$  with  $g$  of `GeoWarp` advantages NFS to estimate more accurate phase shifts and magnitude scales.

## 4.2. Perceptual Evaluation

To measure the perceptual difference of the rendered binaural speeches, we conduct a listening test using multiple stimuli with hidden reference and anchor (MUSHRA). We present nine questions to every nine subjects familiar with the concept of spatial audio. Each question includes the binaural recordings of the benchmark test set as a reference. We instruct participants to rate how similarly spatialized the samples are, compared to the reference sample in a scale from 0 to 1. The samples include hidden references as a high-anchor, and the outputs of the models appear in random permutation order.

Figure 3 shows the MUSHRA scores. We conduct an analysis using multiple posthoc paired t-tests with Bonferroni corrections to reveal the differences between models. We find a significant difference with  $p < 0.005$  between `wo.Shifter` and others including NFS, WarpNet, and BinauralGrad. This again highlights the importance of `Shifter` in NFS. `wo.NI` shows a poor  $\mathcal{L}_{\text{STFT}}$  in Table 1, but according to our posthoc analysis, it is found to have a perceptually insignificant difference between NFS, WarpNet, or BinauralGrad. Although NFS scored worse PESQ in quantitative evaluation, the difference between NFS, WarpNet, and BinauralGrad is found insignificant from our analysis of MUSHRA scores. We conclude that NFS’s capability in modeling ambient noise can be limited, but it is trivial when it comes to spatialization perception.

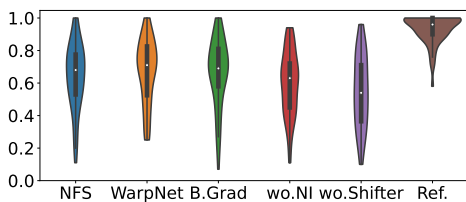


**Fig. 3.** Listening test violin plots. B.Grad denotes BinauralGrad.

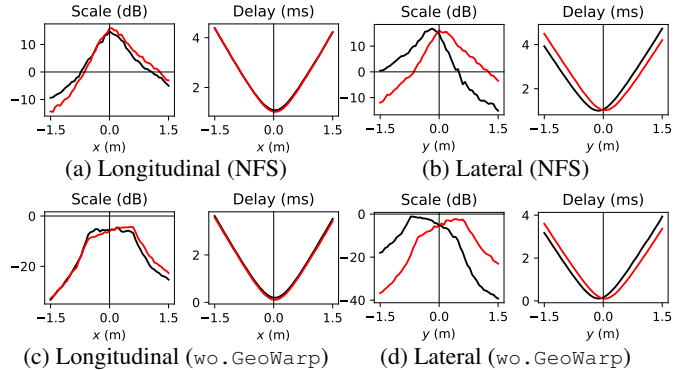


**Fig. 4.** Plot of  $\sigma$  and  $\phi$  averaged over the covering frequencies for the channel with the most dominant intensity. Responses for the left and right channel is colored in black (—) and red (—), respectively.

## 4.3. Efficiency and Interpretability

Besides recording decent performance in quantitative and qualitative evaluations, NFS is highly efficient in memory and computational cost, which is a huge advantage for commodity hardware. Table 2 compares the number of parameters and multiply-accumulates (MACs)<sup>3</sup>, which is a widely used metric to measure the number of computations of a model. Among the comparative models, NFS has the smallest number of parameters, 25 times lighter than BinauralGrad, which consists of a total of 13.8 million parameters. Compared to IR-MLP, our method is lighter and performs better in most objective evaluations. NFS also shows the lightest computational cost. The number of computations required for NFS reaches only 17.8% of that of WarpNet, which is only 1.48% of that of a single denoising step in BinauralGrad (stage1). We do not compare the MACs of IR-MLP as there is no publicly available model.

Estimation within the Fourier space also makes our model easier to interpret. Figure 4 shows the estimated output for the positions along the trajectories parallel to the longitudinal and lateral axes. The delay from NFS is not very different from the geometric delay which is proportional to the Euclidean distance between the source and the receiver. This is natural in that the direct arrivals from the source are the most dominant in their intensity. The scale decreases sharply at locations where the direct path is obscured by the pinna or head. Even without the guidance of `GeoWarp`, our network reflects similar physics in its estimation. This interpretability directly demonstrates how precisely our deep neural network approximates the environment we are trying to simulate and allows us to further compensate for the weaknesses of the model.

## 5. CONCLUSION

We present NFS, a lightweight neural network for binaural speech rendering. Building upon the foundations of the geometric time delay, NFS predicts frame-wise frequency response and phase lags for multiple early reflection paths in the Fourier space. Defined in the Fourier domain, NFS is highly efficient and operates independently of the source domain by its design. Experimental results show that NFS outperforms the previous studies on the benchmark dataset, even with its lighter memory and fewer computations. NFS is interpretable in that it explicitly displays the frequency response and phase delays of each acoustic path, for each source position. We expect improving NFS using generic binaural audio datasets to generalize to arbitrary domains as our future works.

<sup>3</sup><https://github.com/sovrasov/flops-counter.pytorch>

## 6. REFERENCES

- [1] Claudia Hendrix and Woodrow Barfield, “The sense of presence within auditory virtual environments,” *Presence: Teleoperators & Virtual Environments*, vol. 5, no. 3, pp. 290–301, 1996.
- [2] Lord Rayleigh, “Xii. on our perception of sound direction,” *The London, Edinburgh, and Dublin Philosophical Magazine and Journal of Science*, vol. 13, no. 74, pp. 214–232, 1907.
- [3] Donald Wright, John H Hebrank, and Blake Wilson, “Pinna reflections as cues for localization,” *The Journal of the Acoustical Society of America*, vol. 56, no. 3, pp. 957–962, 1974.
- [4] Futoshi Asano, Yoiti Suzuki, and Toshio Sone, “Role of spectral cues in median plane localization,” *The Journal of the Acoustical Society of America*, vol. 88, no. 1, pp. 159–168, 1990.
- [5] Frederic L Wightman and Doris J Kistler, “Headphone simulation of free-field listening. i: stimulus synthesis,” *The Journal of the Acoustical Society of America*, vol. 85, no. 2, pp. 858–867, 1989.
- [6] Henrik Møller, “Fundamentals of binaural technology,” *Applied acoustics*, vol. 36, no. 3-4, pp. 171–218, 1992.
- [7] Lauri Savioja, Jyri Huopaniemi, Tapio Lokki, and Ritta Väinänen, “Creating interactive virtual acoustic environments,” *Journal of the Audio Engineering Society*, vol. 47, no. 9, pp. 675–705, 1999.
- [8] HE Jianjun, Ee Leng Tan, Woon-Seng Gan, et al., “Natural sound rendering for headphones: integration of signal processing techniques,” *IEEE Signal Processing Magazine*, vol. 32, no. 2, pp. 100–113, 2015.
- [9] Dmitry N Zotkin, Ramani Duraiswami, and Larry S Davis, “Rendering localized spatial audio in a virtual auditory space,” *IEEE Transactions on multimedia*, vol. 6, no. 4, pp. 553–564, 2004.
- [10] Jin Woo Lee, Sungho Lee, and Kyogu Lee, “Global hrtf interpolation via learned affine transformation of hyper-conditioned features,” *arXiv preprint arXiv:2204.02637*, 2022.
- [11] Fabian Brinkmann, Alexander Lindau, and Stefan Weinzierl, “On the authenticity of individual dynamic binaural synthesis,” *The Journal of the Acoustical Society of America*, vol. 142, no. 4, pp. 1784–1795, 2017.
- [12] Alexander Richard, Dejan Markovic, Israel D Gebru, Steven Krenn, Gladstone Alexander Butler, Fernando Torre, and Yaser Sheikh, “Neural synthesis of binaural speech from mono audio,” in *International Conference on Learning Representations*, 2020.
- [13] Yichong Leng, Zehua Chen, Junliang Guo, Haohe Liu, Jiawei Chen, Xu Tan, Danilo Mandic, Lei He, Xiang-Yang Li, Tao Qin, et al., “Binauralgrad: A two-stage conditional diffusion probabilistic model for binaural audio synthesis,” *arXiv preprint arXiv:2205.14807*, 2022.
- [14] Wen Chin Huang, Dejan Markovic, Alexander Richard, Israel Dejene Gebru, and Anjali Menon, “End-to-end binaural speech synthesis,” *arXiv preprint arXiv:2207.03697*, 2022.
- [15] Sungho Lee, Hyeong-Seok Choi, and Kyogu Lee, “Differentiable artificial reverberation,” *IEEE/ACM Transactions on Audio, Speech, and Language Processing*, vol. 30, pp. 2541–2556, 2022.
- [16] Israel D Gebru, Dejan Marković, Alexander Richard, Steven Krenn, Gladstone A Butler, Fernando De la Torre, and Yaser Sheikh, “Implicit hrtf modeling using temporal convolutional networks,” in *ICASSP 2021-2021 IEEE International Conference on Acoustics, Speech and Signal Processing (ICASSP)*. IEEE, 2021, pp. 3385–3389.
- [17] Alexander Richard, Peter Dodds, and Vamsi Krishna Ithapu, “Deep impulse responses: Estimating and parameterizing filters with deep networks,” in *ICASSP 2022-2022 IEEE International Conference on Acoustics, Speech and Signal Processing (ICASSP)*. IEEE, 2022, pp. 3209–3213.
- [18] Kurt Hornik, Maxwell Stinchcombe, and Halbert White, “Multilayer feedforward networks are universal approximators,” *Neural networks*, vol. 2, no. 5, pp. 359–366, 1989.
- [19] Michael Mathieu, Mikael Henaff, and Yann LeCun, “Fast training of convolutional networks through ffts,” *arXiv preprint arXiv:1312.5851*, 2013.
- [20] Matthew Tancik, Pratul Srinivasan, Ben Mildenhall, Sara Fridovich-Keil, Nithin Raghavan, Utkarsh Singhal, Ravi Ramamoorthi, Jonathan Barron, and Ren Ng, “Fourier features let networks learn high frequency functions in low dimensional domains,” *Advances in Neural Information Processing Systems*, vol. 33, pp. 7537–7547, 2020.
- [21] Vincent Sitzmann, Julien Martel, Alexander Bergman, David Lindell, and Gordon Wetzstein, “Implicit neural representations with periodic activation functions,” *Advances in Neural Information Processing Systems*, vol. 33, pp. 7462–7473, 2020.
- [22] Zongyi Li, Nikola Kovachki, Kamyar Azizzadenesheli, Burigede Liu, Kaushik Bhattacharya, Andrew Stuart, and Anima Anandkumar, “Fourier neural operator for parametric partial differential equations,” *arXiv preprint arXiv:2010.08895*, 2020.
- [23] Ryuichi Yamamoto, Eunwoo Song, and Jae-Min Kim, “Parallel wavegan: A fast waveform generation model based on generative adversarial networks with multi-resolution spectrogram,” in *ICASSP 2020-2020 IEEE International Conference on Acoustics, Speech and Signal Processing (ICASSP)*. IEEE, 2020, pp. 6199–6203.
- [24] Aaron van den Oord, Sander Dieleman, Heiga Zen, Karen Simonyan, Oriol Vinyals, Alex Graves, Nal Kalchbrenner, Andrew Senior, and Koray Kavukcuoglu, “Wavenet: A generative model for raw audio,” *arXiv preprint arXiv:1609.03499*, 2016.
- [25] Ashish Vaswani, Noam Shazeer, Niki Parmar, Jakob Uszkoreit, Llion Jones, Aidan N Gomez, Lukasz Kaiser, and Illia Polosukhin, “Attention is all you need,” in *Advances in neural information processing systems*, 2017, pp. 5998–6008.
- [26] Jie Hu, Li Shen, and Gang Sun, “Squeeze-and-excitation networks,” in *Proceedings of the IEEE conference on computer vision and pattern recognition*, 2018, pp. 7132–7141.
- [27] Hanxiao Liu, Zihang Dai, David So, and Quoc V Le, “Pay attention to mpls,” *Advances in Neural Information Processing Systems*, vol. 34, pp. 9204–9215, 2021.
- [28] Liyuan Liu, Haoming Jiang, Pengcheng He, Weizhu Chen, Xiaodong Liu, Jianfeng Gao, and Jiawei Han, “On the variance of the adaptive learning rate and beyond,” *arXiv preprint arXiv:1908.03265*, 2019.